

E-band active Q-enhanced pseudo-combine resonator in 130nm SiGe BiCMOS

Nishant Singh (ORCID: 0000-0003-0609-1145)
and Tinus Stander* (ORCID: 0000-0003-1600-6135)

Carl and Emily Fuchs Institute for Microelectronics
Dept. EEC Engineering
University of Pretoria
South Africa

*Corresponding author. Tel.: +27-12-420-6704. E-mail address: tinus.stander@up.ac.za

Abstract. We present an active Q-enhanced pseudo-combine resonator integrated in 130nm SiGe BiCMOS. It is shown that the resonator Q_0 can be enhanced, controllably, from 15 to 1578 at 78.8 GHz through application of a SiGe HBT-based negative resistance circuit. This is the first time that resonator Q-enhancement is demonstrated experimentally in silicon above 40 GHz, and the first time negative enhancement with single-ended pseudo-combine loading is used.

Keywords: BiCMOS integrated circuits, heterojunction bipolar transistors, millimeter wave integrated circuits, Q measurement, resonators

1 Introduction

The millimeter-wave spectrum (30 – 300 GHz), and in particular the lightly licensed E-band (60 – 90 GHz), offers significant unused spectrum for automotive RADAR and communications backhaul applications [1]. Although the development of deep submicron nodes in CMOS and SiGe BiCMOS [2] have led to commercially feasible mm-wave front-ends suitable for system-on-chip (SoC) integration [3], there is still no compact, low-loss solution to effective channelization on-chip. Full SoC integration of front-end filters is hampered by the low attainable quality factors (Q-factors) of on-chip distributed passives [4], which reduces filter selectivity and increases insertion loss [2]. For this reason, front-end filters are currently omitted from SoCs [5, 6], and no E-band equivalents exist to ultra-compact SAW or BAW off-chip RF and microwave filters. In addition, having filters on-chip would allow the SoC designer greater design flexibility to trade-off, for example, minimum noise figure (NF) and out-of-band suppression (with implications to image rejection or

saturation) by changing the order of the filter and the LNA in the receiver.

One possible remedy is the adoption of active Q-enhancement of passive resonators on-chip [7–11], at the expense of potentially higher NF and finite dynamic range. A secondary goal would be to minimize the size of the distributed components (thereby saving on chip area) by opting for pseudo-combine resonators [12] as opposed to full quarter-wave ($\lambda_g/4$) or half-wave ($\lambda_g/2$) resonators.

Negative resistance based Q-enhancement on-chip has been applied in GaAs at 65 GHz using $\lambda_g/4$ coplanar waveguide (CPW) resonators [7], as well as at 22.6 GHz [8] with lumped resonators. Both enhancement circuits feature inductive input reactance due to inductive feedback, where capacitive reactance is required for the synthesis of combine filters [12]. In CMOS, active Q-enhancement has been demonstrated at 34.2 GHz [9] and 25.65 GHz [10] on $\lambda_g/2$ complementary conducting strip (CCS) transmission line resonators, though in both cases the choice of cross-coupled enhancement circuit rules out the use of more compact $\lambda_g/4$ resonators. The lumped resonators in [11] were enhanced at 24 GHz using the lumped inductor itself as feedback element in the circuit, which also makes the single-ended input impedance inductive.

An unexplored avenue for mm-wave resonator Q-enhancement on-chip is the application of single-ended Colpitts-type negative resistance circuits [3, 13]. In addition to the negative resistance, the capacitive feedback (exploiting the availability of high quality MIM capacitors in CMOS BEOL) would provide capacitive input reactance, thereby aiding in the synthesis of compact pseudo-combine filters if a single-ended topology is used.

In this letter, we present measurement results of an active Q-enhanced E-band pseudo-combine resonator, implemented with SiGe HBTs from the GlobalFoundries US 8HP 130nm SiGe BiCMOS process. This is the first time that Q-enhancement of passive resonators in CMOS is presented above 40 GHz, and the first time that an active Q-enhanced pseudo-combine resonator is published.

2 Circuit model and layout

The negative resistance is generated by a single HBT in common collector configuration [3], as shown in Fig. 1. Q_1 is an HBT of $2.5 \times 0.12 \mu\text{m}$. C_1 and C_2 are identical 17 fF MIM capacitors, and R_1 is a 495 Ω TaN BEOL resistor. The circuit is biased with fixed V_1 at the collector and variable V_2 (through an unshielded inductive line L_1 of $4 \times 650 \mu\text{m}$ on the top metal AM acting as RF choke) at the base in order to control collector current I_C and, consequently, the achieved negative resistance. C_3 is a 464 fF MIM capacitor used to provide an AC ground, bypassing the DC probe and off-chip cable inductance L_C . The negative resistance circuit is capacitively coupled to the resonator through C_4 , a 200 fF MIM capacitor.

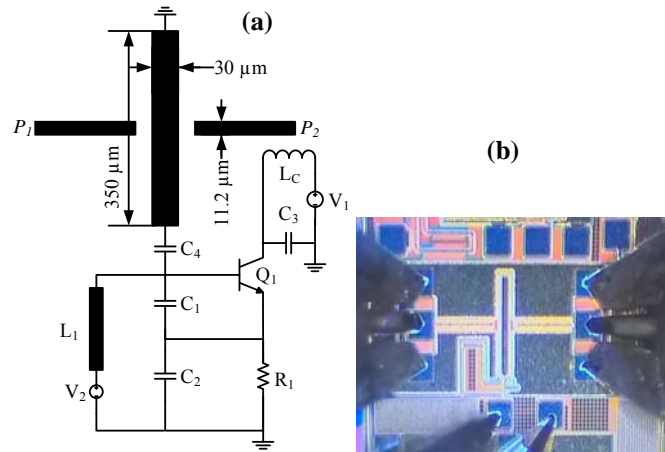


Fig. 1. a Active Q-enhanced resonator circuit diagram
b Micrograph of circuit under test

The resonator itself is a microstrip pseudo-combine resonator, implemented using the top two AM and MQ metal layers of the BEOL. The $350 \times 30 \mu\text{m}$ resonator is grounded on one end using a $29.1 \times 6.5 \mu\text{m}$ via array stack between AM and MQ. The resonator is weakly coupled to input and output 50Ω feed lines over a $30 \mu\text{m}$ gap.

3 Measurement results

The transmission response of the circuit is shown in Fig. 2(a). Q_0 is extracted from two-port S-parameters using the method in [14], and is found to be tunable up to 1578 at an f_0 of 78.8 GHz for an I_C of 3.44 mA (equating to a negative resistance of -6Ω) whilst remaining stable. For comparison, the response of an identical unenhanced combline resonator loaded with a 19 fF MIM capacitor is also shown in Fig. 2, achieving a Q_0 of only 15. It is observed in Fig. 2(b) that increasing I_C enhances Q_0 up to a critical point beyond which enhancement is reduced, similar to what is observed in [7].

Because the resonator is weakly coupled to the ports, the NF response is dominated by the attenuation of the coupling, making it impossible to make a meaningful Y-factor measurement. Similarly, the high attenuation makes resonator immune to compression for practical values of E-band power sources.

When compared to state-of-the-art in active Q-enhanced resonators above 20 GHz (Table 1), it is evident that this is the first resonator circuit of its type in SiGe BiCMOS and the first in E-band. The enhancement is achieved at the expense increased power consumption P_{diss} , though the Q-tunability demonstrated in Fig. 2(b) could be used as a trade-off between P_{diss} and Q_0 . It is also the first to use capacitive feedback in a single-ended enhancement.

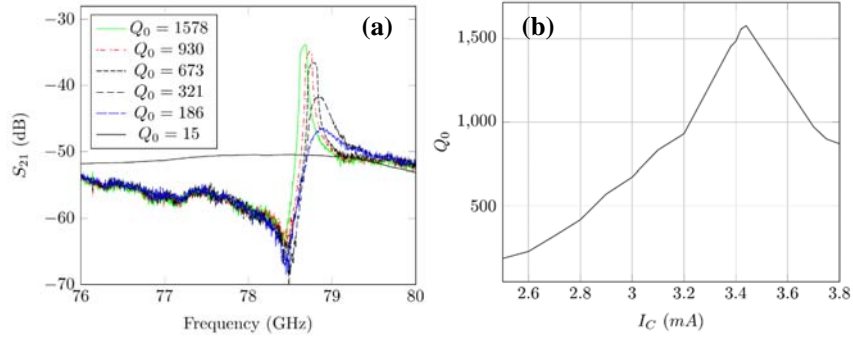


Fig. 2. **a** Transmission response of active Q-enhanced resonator at various enhancement levels. **b** Q_0 tuning for different values of I_C .

Table 1. Comparison of MMIC Q-enhanced resonators above 20 GHz

| Ref. | Process | Resonator, Enhancement | R_N (Ω) | f_0 (GHz) | Q_0 | P_{diss} (mW) |
|-----------|------------|--------------------------------------|--------------------|-------------|-------|------------------------|
| [7] | 150nm GaAs | $\lambda/4$ CPW, single-ended | -2 | 65 | N/A | N/A |
| [9] | 180nm CMOS | $\lambda/2$ CCS, cross-coupled | N/A | 34.2 | N/A | 1.85* |
| [10] | 180nm CMOS | $\lambda/2$ CCS, cross-coupled | -146* | 25.65 | 513 | 0.67 |
| [11] | 180nm CMOS | Lumped, single-ended | -7.55* | 24 | 46.1 | 2.1* |
| This work | 130nm SiGe | $\lambda/4$ microstrip, single-ended | -6 | 78.8 | 1578 | 12 |

*Values estimated

4 Conclusion

It is demonstrated, for the first time, that a Q-tunable high- Q_0 pseudo-combline resonator can be realized in a SiGe BiCMOS process using a BEOL microstrip line and an HBT-based negative resistance circuit. Future work will include application of frequency agility through implementation of varactors, as well as application in a full frequency agile filter. The effect of active Q-enhancement on linearity and NF will also be investigated using resonators with stronger source and load coupling.

Acknowledgements

This work was supported by the National Research Foundation under grant UID 93921, as well as the Eskom Tertiary Education Support Programme (TESP) and the UNESCO Participation Programme. The authors wish to thank the MOSIS Educational Programme (MEP) for the sponsored prototyping run on the GFUS 8HP process.

References

1. Stander T (2015) A review of key development areas in low-cost packaging and integration of future E-band mm-wave transceivers. In: AFRICON 2015. IEEE, Addis Ababa, Ethiopia, pp 1–5
2. Long J, Chan W, Zhao Y, Spirito M (2011) Silicon VLSI catches the millimeter wave. *IEEE Commun Mag* 49:182–189 . doi: 10.1109/MCOM.2011.6035834
3. Jain V, Javid B, Heydari P (2009) A BiCMOS Dual-Band Millimeter-Wave Frequency Synthesizer for Automotive Radars. *IEEE J Solid-State Circuits* 44:2100–2113 . doi: 10.1109/JSSC.2009.2022299
4. Stander T (2014) A comparison of basic 94 GHz planar transmission line resonators in commercial BiCMOS back-end-of-line processes. In: 2014 International Conference on Actual Problems of Electron Devices Engineering (APEDE). IEEE, pp 185–192
5. Trotta S, Sapone G, Jungmaier RW, Chakraborty A, Bal JS, Knapp H, Forstner H-P, Ismail N, Wojnowski M, Seler E, Mousavi MP, Malsam D (2014) A V and E-band packaged direct-conversion transceiver chipset for mobile backhaul application in SiGe technology. In: 2014 11th European Radar Conference. IEEE, pp 352–355
6. Kucharski M, Kissinger D, Ng HJ (2018) A universal monolithic E-band transceiver for automotive radar applications and V2V communication. In: 2018 IEEE 18th Topical Meeting on Silicon Monolithic Integrated Circuits in RF Systems (SiRF). IEEE, pp 12–14
7. Ito M, Maruhashi K, Kishimoto S, Ohata K (2004) 60-GHz-Band Coplanar MMIC Active Filters. *IEEE Trans Microw Theory Tech* 52:743–750 . doi: 10.1109/TMTT.2004.823531
8. Kang-Wei Fan, Ching-Chih Weng, Zou-Min Tsai, Huei Wang, Shyh-Kang Jeng (2005) K-band MMIC active band-pass filters. *IEEE Microw Wirel Components Lett* 15:19–21 . doi: 10.1109/LMWC.2004.840961
9. Meng-Ju Chiang, Hsien-Shun Wu, Tzuang CC (2008) A 3.7-mW zero-dB fully integrated active bandpass filter at Ka-band in 0.18-um CMOS. In: 2008 IEEE MTT-S International Microwave Symposium Digest. IEEE, pp 1043–1046
10. Kuo-Ken Huang, Meng-Ju Chiang, Tzuang C-KC (2008) A 3.3 mW K-Band 0.18-

- um 1P6M CMOS Active Bandpass Filter Using Complementary Current-Reuse Pair. *IEEE Microw Wirel Components Lett* 18:94–96 . doi: 10.1109/LMWC.2007.915035
11. Wang S, Huang B-Z (2012) Design of a Low-Loss and Highly-Selective CMOS Active Bandpass Filter at K-Band. *Prog Electromagn Res* 128:331–346 . doi: 10.2528/PIER12031301
 12. Sanchez-Renedo M (2007) High-Selectivity Tunable Planar Compline Filter With Source/Load-Multiresonator Coupling. *IEEE Microw Wirel Components Lett* 17:513–515 . doi: 10.1109/LMWC.2007.899313
 13. Ying Chen, Mouthaan K, Geurts M (2010) A wideband Colpitts VCO with 30% continuous frequency tuning range using a tunable phase shifter. In: 2010 IEEE International Conference of Electron Devices and Solid-State Circuits (EDSSC). IEEE, pp 1–4
 14. Bray JR, Roy L (2004) Measuring the unloaded, loaded, and external quality factors of one- and two-port resonators using scattering-parameter magnitudes at fractional power levels. *IEE Proc - Microwaves, Antennas Propag* 151:345 . doi: 10.1049/ip-map:20040521